Bulletin of Earthquake Engineering
https://doi.org/10.1007/s10518-022-01319-w

ORIGINAL ARTICLE

Numerical simulation of RC frames infilled with RC walls for seismic strengthening of existing structures

Elpida Georgiou[1] · Nicholas Kyriakides[1] · Christis Z. Chrysostomou[1]

Received: 24 June 2021 / Accepted: 6 January 2022

Abstract

Although it is evident that the RC infill wall is an economic and practical way to improve the lateral strength of framed structures and a retrofitting method for existing buildings to withstand earthquake loads, there are still a lot of limitations regarding their application. Codes do not provide any guidance for their design and detailing or specific regulations for their interaction with the bounding frame. Furthermore, specific directions do not exist for the modelling or evaluation of frame bays converted into RC walls, depending on the type and details of the connection. A representation of the real behaviour of the wall and its interaction with the bounding frame during an earthquake is necessary to provide more accurate guiding information. For this aim, numerical models of this structural system were developed and are presented in this paper. The experimental results of the project SERFIN, which was a full-scale four-storey model tested with the pseudo-dynamic method at the ELSA facility of the Joint Research Centre in Ispra, were used to calibrate the numerical models. Two-dimensional (2D) frames were modelled in DIANA FEA, and nonlinear transient analyses were performed to simulate the experimental results obtained from the SERFIN full-scale experiment. In this paper, the FE model simulation of the test specimen is presented along with a comparison between the experimental results and the numerical ones. It was concluded that the developed numerical models capture effectively the behaviour of the studied structural system and can be used for parametric studies to examine the effects of the number of dowels on the behaviour of the system and propose design guidelines based on the results of the parametric study.

Keywords Seismic strengthening of structures · RC infill walls · Modelling of dowels · Finite element model

✉ Elpida Georgiou
es.georgiou@edu.cut.ac.cy

[1] Department of Civil Engineering and Geomatics, Cyprus University of Technology, 3036 Limassol, Cyprus

Published online: 15 January 2022

1 Introduction

In recent decades, low and medium-rise RC buildings have experienced considerable damage during earthquakes, which resulted in casualties and financial loss. Thereafter, many damaged existing buildings had to be effectively and economically retrofitted. Various strengthening techniques have been assessed and applied in the past decades for the rehabilitation of such existing RC frames. Most of the strengthening techniques interrupt the everyday life of residents, who must evacuate the building during the intervention. Nowadays, most of the strengthening procedures are based on global strengthening schemes and the structures are usually strengthened for limiting lateral displacements to compensate for low ductility (Kaplan et al. 2011; Moehle 2000; Sonuvar et al. 2004). Increasing the global stiffness and reducing the seismic deformation expectations of a building for the aim of seismic retrofitting may be more cost-effective in comparison with the local intervention of existing components in order to strengthen their capacities (Fardis 2009).

As many RC frame structures with non-seismic details have been severely damaged, many researchers (Agarwal and Shrikhande 2006; Almusallam and Al-Salloum 2007; Baran and Tankut, 2011; Frosch, 1996, 1999; Koutas et al. 2015; Ozden et al. 2011) have investigated the infill-wall strengthening-method to improve seismic performance by inserting cast-in-place concrete or precast (PC) walls inside the beam-column frame structure. The strengthening of damaged RC buildings by infilling selected bays in both directions of the frames with RC infill walls, especially on the perimeter, has proved to be one of the most feasible approaches in the seismic strengthening of existing buildings. The infill-wall strengthening-method is cost effective, while greatly increasing shear strength (Choi et al. 2020). This is a popular, simple, effective, and economic strengthening method of improving the overall behaviour or RC buildings and is preferred when there are too many members to be retrofitted (Choi et al. 2020; Turk et al. 2006; Kaplan et al. 2011; Fardis et al. 2013). According to Chrysostomou et al. (2013a) this is the most effective and economic method for retrofitting multi-storey multi-bay RC buildings, especially those with pilotis (soft-storey). This method can be applied to increase the stiffness, strength, and ductility of the building. Also, with the full infill of selected bays of an existing RC frame, the effectiveness of the retrofitting is increased, and the construction cost is reduced. However, it is not easy to secure the sufficient shear resistance performance of the connection due to the complex connection details between the RC frame and the infill wall (Choi et al. 2020). The RC infills as a retrofitting method is commonly applied to guarantee monolithic behaviour between the old and the new members to design the new RC walls according to the codes (CEN 2010; KANEPE 2017). Also, Jirsa (1988) states that the new materials must be attached to the existing structure to provide the type of monolithic action generally assumed in the design of the retrofit scheme and states that a simple method to make the attachments involves the use of epoxy resins to grout reinforcing bars into the existing concrete elements. The monolithic behaviour is achieved by the construction of a new thicker web than the beams and the columns of the existing frame panel with the location of the new reinforcement outside the existing members and the details of reinforcement as in a new wall (Fardis et al. 2013). In this way, the new infill walls are much stronger than what is needed for the strengthening of the structure, and this 'over-strength' causes additional issues like the weak foundations of the existing building compared to the new wall (Fardis et al. 2013). However, the addition of RC infill walls with the same thickness as the members of the frame that bound the new wall for the seismic strengthening of RC buildings is a relatively new method.

Even though the RC infills is a common retrofitting method and it is extensively applied to guarantee monolithic behaviour between the old and new members, it is not addressed quantitatively by the codes, not even by EC8-3. The retrofitting guidelines of Greece (KANEPE 2017) refer to the introduction of RC infills within a frame, just in terms of forces, providing tools for calculating their yield and failure deformations and stiffness, only if they are integral with the bounding frame. Although for other strengthening methods of existing structures there are guidelines regarding the design of retrofit and certain aspects of the seismic response of the retrofitted structure, there are still open topics about the retrofit method studied in this work. Specifically, their interaction with the bounding frame, their design, and the detailing between the new web and the bounding frame members need to be studied and regulated.

According to EC8-3, among other intervention methods, the addition of new structural elements is mentioned (e.g., bracings or infill walls). There are instructions for the design of the structural intervention and the retrofit design procedure. In EC8-3 there are capacity models for the assessment for the existing members of the structure under flexure, and capacity models for strengthening with concrete jacketing, with steel jacketing, and with Fibered Reinforced Polymers (FRP) plating and wrapping. For the addition of new RC walls within existing RC frames, there are no models in EC8-3 (CEN 2010). As it was mentioned above, the only way to design the new RC wall according to EC8-3 is by the full monolithic action between the old and the new members.

On the other hand, KANEPE (2017) refers to the introduction of RC infills within an existing frame. More specifically, this method is recommended for the installation of RC walls for selected frames for the systematic increase of the stiffness and the seismic capacity of the structure. The new members should be connected properly to the existing frame and must have a safe foundation. During the analysis of the new structure, the rotation of the foundation of the new wall should be considered. The new RC wall can be constructed in situ or can be precast. KANEPE refers to the design of such walls only in terms of forces, providing tools for calculating their deformations at yield, failure, and stiffness only if they are integral with the bounding frame.

American Society of Civil Engineers (2007) addresses frames with concrete infills with no special provisions for continuity from storey to storey and it considers the concrete of the infill separately from the concrete of the frame. However, the American Society of Civil Engineers (2007), adds that when the frame and the concrete wall are assumed to act as a monolithic wall, flexural strength shall be based on continuity of vertical reinforcement in both the column acting as boundary components and the infill wall, including anchorage of the infill reinforcement in the boundary frame. Nevertheless, it does not provide any guidance for such continuity or anchorage, neither on how to determine key properties of the monolithic wall depending on the connection of the RC infill with the surrounding frame.

The inadequacy of design codes in this respect is due to the lack of knowledge of the behaviour of walls created by the infilling of a bay of an existing RC frame. Furthermore, regulations do not exist for modelling or assessment of frame bays converted into RC walls depending on the details and type of the connection. Many different types of connections of the infill wall to the surrounding frame have been studied, such as the performance of different types of shear keys, dowels, and chemical anchors and wall reinforcement configurations (Altin et al. 1992; Aoyama et al. 1984; Frosch et al. 1996; Jirsa 1988; Sugano 1980). The design of new RC infill walls and the contribution of the dowels that connect the new infill wall to the existing RC frame are topics that need further study. There is no quantitative procedure for the design and construction of the new walls. In addition, the contribution of dowels that connect the new infill wall to the surrounding frame members has not been analysed adequately yet. The dowels affect the behaviour of RC infills and the overall shear resistance capacity of the building. Their action is a complicated mechanism, and the way of designing them is not clear. The only way to design the new RC walls according to EC8-3 is to guarantee monolithic behaviour between the old and new concrete. Although for other strengthening methods of existing structures there are guidelines regarding the retrofit design and certain aspects of the seismic response of the retrofitted structure, there are still open issues about the studied retrofit method. For example, their interaction with the bounding frame, as well as their design and detailing between the new web and the surrounding frame members need to be regulated. Further research should include experimental investigations focused on the behaviour of strengthened structures, as well as methods of establishing the connection between the old and newly designed elements (Folici 2015). Guidelines have been lacking beyond the epoxy manufacturer's recommendations on details of installing epoxy grouted dowels and design values to use (Wyllie 1988). Frequently, it is necessary to strengthen existing concrete structures for improved seismic performance, either after a damaging earthquake or in preparation for a future event. Epoxy grouted dowels are ideal for this task due to the strength and ease of installation of epoxy resins to anchor dowels (Wyllie 1988).

Moreover, the experimental research work that has been performed in the last decades on the application of RC infill walls is not adequate and most of the research has mostly targeted what is feasible: testing of one-to-two storey specimens because of the practical difficulties of testing large specimens with high resistance (Chrysostomou et al. 2016). The tests have been restricted to small-scale specimens, possibly owing to the technical limitations of testing walls of very large shear force resistance (Chrysostomou et al. 2013a; Fardis et al. 2013). Another drawback of past investigations is that they did not propose or even follow a quantitative procedure for the design of the connection between the RC infilling and the bounding members of the frame. Furthermore, they have not led to, or supported, any procedure for the quantification of the engineering properties of the RC infilled frame, which is crucial for its analysis and design in the context of modern performance-based seismic design, that is the moment, the effective stiffness, and shear resistances, the deformation at yielding and the cyclic deformation capacity (Strepelias et al. 2012). Subsequently, data is missing for full-scale specimens that reflect actual cases.

Despite the common field practice of new walls that encapsulate the frame members, the tests have been limited to small-scale specimens with new webs thinner than the surrounding beams or columns, possibly owing to the technical limitations of testing walls of very large shear force resistance (Chrysostomou et al. 2013a; Fardis et al. 2013). From the experimental studies that were studied, only the SERFIN experiment was full scale. Most of the experiments were on scales 1:3, 1:5, and 1:7, and only a few on a 1:2 scale. In addition, it was noted that most of the experiments were testing one to three-storeys and just one was found to test five storeys, but even though they examined the effect of the number of storeys, they did not examine the number of bays. Most of the specimens were one-bay ones and very few specimens were three-bay. It is apparent that for practical reasons, the experimental research mainly targets what was feasible and not on what is realistic and what is found in practice. Even in the extensive research on this subject, there is no experimental data for the taller full-scale specimens that reflect real building applications probably due to the practical difficulties associated with the high forces needed for the tests (Chrysostomou et al. 2013a). A common feature of all tests is the rather small thickness of the RC infill compared to the width of the frame members. This further penalizes the shear resistance of the composite wall and the new web-frame connection (Strepelias et al. 2012).

Another drawback that was noted from the past investigations is that they did not propose or even follow a quantitative procedure for the design of the connection between the RC infilling and the surrounding frame members. That detail was empirically selected, almost non-engineered (Fardis et al. 2013). Furthermore, they have not led to, or supported, any procedure for the quantification of the engineering properties of the RC infilled frame which is essential for this analysis and design in the context of modern performance-based (and most often displacement-based) seismic design: the effective stiffness, the moment and shear resistances, the deformation at yielding and the cyclic deformation capacity (Strepelias et al. 2012). Nevertheless, it is evident from the research that the RC infill walls is an economic and practical way to strengthen the lateral stability of framed structures and to retrofit existing buildings to withstand earthquake loads.

To start filling the gap of knowledge and to examine the effectiveness of seismic retrofitting of multi-storey multi-bay RC frame buildings by the conversion of selected bays into new walls through RC infilling, a full-scale specimen was studied experimentally through pseudo-dynamic (PsD) tests within the project “Seismic Retrofitting of RC Frames with RC Infilling” (SERFIN) at the European Laboratory of Structural Assessment (ELSA) facility at the Joint Research Centre (JRC), in Ispra. The purpose was to study the efficiency of the retrofitting method through experimental testing of a full-scale model of four-storeys with the PsD method. The frames of the SERFIN model were designed and detailed for gravity loads only. Several connection details between the new RC infill walls and the surrounding frame were used. Further details and information about this research work can be found in Chrysostomou et al. (2013a), Chrysostomou et al. (2013b), Chrysostomou et al. (2014), Poljansek et al. (2014).

It is apparent that the codes and standards for seismic retrofitting of existing RC structures do not provide complete guidance for the design and detailing of the attachment of new walls to existing frames. Furthermore, regulations or even design guidelines do not exist for modelling or evaluation of frame bays converted into RC walls depending on the type and details of the connection. Subsequently, further investigation is required regarding their design and construction, and a parametric study of dowels is necessary. In order to achieve the above objectives two actions are necessary: first, sophisticated and reliable nonlinear numerical models are required that capture the complex behaviour of such a system, and second, parametric studies, using the calibrated model of the first action, in which the effects of the reduction of dowels are studied and design guidelines are proposed.

In this paper, the FE model simulation of the test specimen is presented along with a comparison between the experimental results of the SERFIN project and the numerical ones, both at local and global level, which covers the first action. Detailed description of the experimental results are given in Chrysostomou et al. (2013a), Chrysostomou et al. (2013b), Kyriakides et al. (2015), Chrysostomou et al. (2014), Poljansek et al. (2014). The development and calibration of the numerical models are presented in Sects. 2 and 3, respectively, while in Sect. 4 the conclusions drawn are stated.

2 Numerical simulation

In order to fulfil the first action of this research, FE models of the SERFIN full-scale PsD tested specimen were developed in the DIANA FEA tool and were validated using the experimental results of the test.

In this section, the FE model of the south frame of the SERFIN, and its calibration are described and presented.

2.1 Finite element model simulation in DIANA FEA

In this section, the simulation of the south frame of the SERFIN prototype specimen model in DIANA FEA is presented. The numerical models that were developed are2D continuum FE models. The assumptions and the boundary conditions that were made for the development of the FE models, the elements, and the constitutive material laws that were selected from the DIANA FEA library, and the mesh that was generated are presented. In addition, the loads that were applied to the models and the analysis procedures used are described.

Much of the focus was on the behaviour of the individual models that were used for the modelling and how they were validated, so they would correctly reflect the overall model behaviour. Suitable elements for the simulation of the RC infills, reinforcement, and frame members were selected along with material models for concrete and reinforcement, which included hysteretic behaviour with strength and stiffness degradation. In this way, the FE models consider the nonlinear hysteretic behaviour of materials during a seismic excitation to capture and evaluate the behaviour of RC infills. The mechanical characteristics of the materials of the model have been chosen with a correlation with the experimental characteristics as discussed in Sect. 2.1.3. Furthermore, a detailed analysis was obtained considering the nonlinear behaviour of the materials at the local level (nonlinear transient analyses were performed) to simulate the experimental results.

Two distinct numerical models were developed in DIANA FEA and they consisted of the existing RC frame and the new RC infill wall, like the prototype model. Initially, the first numerical model was developed without the consideration of the interaction between the existing bounding frame and the new RC wall (model I displayed in Fig. 3). The infills were monolithic with the bounding frame and all reinforcing bars were modelled to carry axial loads only. In the second numerical model (model II shown in Fig. 4), the interaction between the existing bounding frame and the new RC wall was modelled through interface elements, to allow for the separation of the bounding framing members and the RC wall at the interface when they are in tension (caption of tension cut-off behaviour). In this case, the dowels were modelled in such a way so they can take shear and axial forces, as well as moments. Both numerical models are described and presented along with their results in this section.

2.1.1 Model characteristics and assumptions

The boundary conditions and assumptions that were made for the simulation and the analysis of the FE model are described in this section. Specifically, a rigid foundation was simulated, and pin supports (X and Y translational constraints) were applied at the base of the building model (see Fig. 1). Moreover, the additional retrofit with three-sided carbon fiber reinforced polymers (CFRPs) jackets that were applied at the SERFIN specimen to reinforce the edges of the wall on the lap-length to avoid premature tensile lap-splice failure (for further details see Chrysostomou et al. (2013a), Chrysostomou et al. (2013b); Kyriakides et al. (2015), Chrysostomou et al. (2014), Poljansek et al. (2014) were not considered in the DIANA FE model. In Figure 1 the geometries of concrete and reinforcement members in DIANA FEA are illustrated.

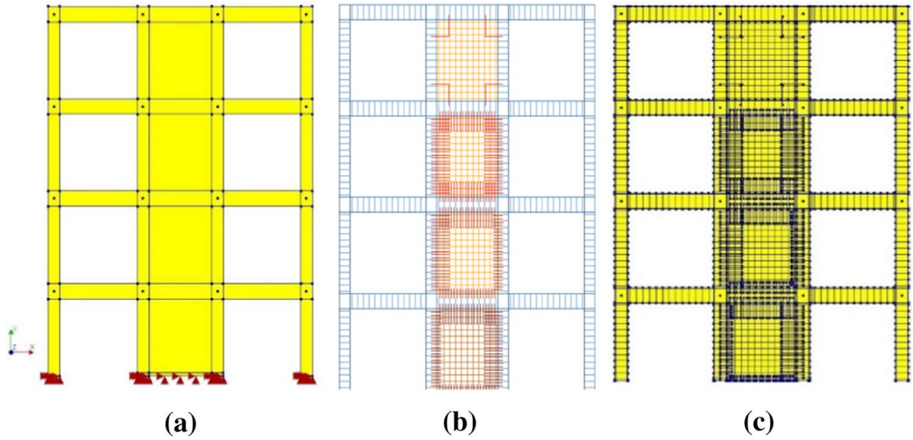

Fig. 1 **a** Concrete geometry shapes of the FE model and boundary conditions, **b** Embedded reinforcement bars for the existing frame and web reinforcement of the infill wall and dowels, **c** Complete geometry of the FE model

The additional weight of half of the experimental slab and transverse beams was added to the 16 joints of the model through mass point elements. The dead and live loads were applied on the beams as edge pressure load with the same values as the prototype model and the earthquake signal with 0.25 g peak acceleration was added as body force for base excitation with the earthquake time-history function.

Then, the nonlinear transient analysis was executed in DIANA FEA. In order to perform a nonlinear transient analysis, the Rayleigh damping coefficients were defined in DIANA FEA using a 0.25% damping ratio, which is a small value since the SERFIN specimen was tested using the pseudo-dynamic (PsD) test method in which no damping is applied. The secant Newton method (quasi-newton), which is an iterative method, was applied, together with the line search method. The convergence tolerance that was applied was 0.2% for both force and displacement.

2.1.2 Elements and mesh

The elements and the mesh that were selected and applied for all the members of the frame in DIANA FEA are presented in this section. Different elements were used to simulate the concrete elements of the frame, the frame reinforcement, the web reinforcement of the infill, the dowels that connect the new infill wall to the existing frame, and the interface between the existing frame and the new infill walls. In addition, as was mentioned before, point mass elements were used to add half the mass of the specimen (slabs and transversal beams, Poljansek et al. (2014) to the 2D FE frame.

It is important to mention that for the second FE model (model II) reinforcing bars of the RC frame and the web reinforcement of RC infills were modelled to carry only axial loads, whereas the dowels were modelled to capture not only axial loads but shear and moment as well.

2.1.2.1 Concrete mesh The concrete frame members (columns, beams, and joints) and the infill wall were simulated using the 2D regular plane stress quadrilateral elements with 8

Table 1 Reinforcing bars for the frame members

Frame members	Longitudinal reinforcing bars	Shear links
Longitudinal beams	4Y12 Up + down	Y8/200
Columns	4Y20	Y8/200

Table 2 Infill wall reinforcing web bars

Infill wall	Vertical web bars	Horizontal web bars
Ground floor web bars	Y10/200# (2 × 11 bars)	Y10/200# (2 × 13 bars)
1st storey web bars	Y8/200# (2 × 11 bars)	Y8/200# (2 × 13 bars)
2nd storey web bars	Y8/200# (2 × 11 bars)	Y8/200# (2 × 13 bars)
3rd storey web bars	Y8/200# (2 × 11 bars)	Y8/200# (2 × 13 bars)

nodes (CQ16M) from the DIANA FEA element library. In addition, the plane stress elements can be combined with the bond-slip reinforcement elements in DIANA FEA in case we do not want perfect bonding between concrete and reinforcement steel (DIANA FEA BV 2019).

2.1.2.2 Reinforcement mesh For the first FE model (model I) the frame reinforcing bars, the web reinforcement of the RC infills, and the dowels were modelled as reinforcement steel bars and for their mesh, 1D embedded bar reinforcement inside plane stress elements were used, which can carry only axial loads and they exhibit strains and stresses in the longitudinal direction only. For model II, only the frame reinforcing bars and the web reinforcement of the RC infills were modelled with these elements, since the dowels were modelled in such a way so they can take not only axial load but also shear load and bending moment. The reinforcement steel bar elements that were applied for the reinforcement in the two developed models are described in this section.

Reinforcement steel bar elements can be embedded in all structural interface elements, and they are applied when it continues from one structural part into another and have a considerable effect on the cracking or sliding of the connection between these two parts. Such reinforcement was applied in the FE model that was generated. For the generated FE models, the bar reinforcement is embedded in the regular plane stress elements that were used for the concrete members of the FE model. For the FE model of the south wall that is examined, four cross-section areas of bars (Y8, Y10, Y12, Y20) were used like in the prototype model (Poljansek et al. 2014). The reinforcing bars that were applied in the FE models are given in Tables 1, 2, 3 and 4.

2.1.2.3 Dowel mesh As it is shown from the literature, even though the dowel reinforcing bars (shear connectors) between the existing bounding frame members and the new infill wall affect the behaviour of RC infills and the overall shear resistance capacity of a building, it is not clear how to design them. This is because their behaviour is based on a complicated mechanism. The modelling of the dowel action has not been mentioned in the literature for the finite element (FEM) analysis before 1991 (El-Ariss 2007). To analyse the details of the dowel action, the steel bars need to be individually modelled by finite elements and a very fine mesh must be used for concrete. Except for a large

Table 3 FE model dowel bars

	Vertical dowels-connecting beams		Horizontal dowels-connecting columns	
	West side	East side	Down	Up
Ground floor infill wall (W1)	24Y20/100 (l = 320 mm)	24Y20/100 (l = 660 mm)	20Y20/100 (l = 320 mm)	20Y20/100 (l = 660 mm)
1st storey infill wall (W2)	24Y18/100 (l = 545 mm)	24Y28/100 (l = 290 mm)	20Y18/100 (l = 290 mm)	20Y18/100 (l = 545 mm)
2nd storey infill wall (W3)	24Y16/100 (l = 530 mm)	24Y18/100 (l = 530 mm)	20Y16/100 (l = 530 mm)	20Y16/100 (l = 530 mm)
3rd storey infill wall (W4)	2Y16 (l = 530 mm)	2Y16 (l = 530 mm)	2Y16 (l = 530 mm)	2Y16 (l = 530 mm)

Table 4 FE model starter bars

Starter bars	West column	East column	Foundation beam	Storey beam
Ground floor infill wall (W1)	2 × 13Y10/200 (l = 670 mm)	–	2 × 11Y10/200 (l = 670 mm)	–
1st Storey infill wall (W2)	–	2 × 13Y18/200 (l = 520 mm)	2 × 11Y18/200 (l = 520 mm)	–

number of the finite elements, individual modelling of the steel bars and concrete is not compatible with the common practice of modelling the concrete and steel together in the analysis of RC structures. In experimental tests, the shear force transferred by the dowel action is quite difficult to measure because it is embedded with other shear transfer components (El-Ariss 2007). In fact, since the dowel action involves interaction between the reinforcement bars and the concrete near the cracks and the interaction stresses are extremely difficult to measure, many details of the dowel action have never been investigated (El-Ariss 2007). There are not adequate experimental data or theoretical analysis for the dowel action near the peak load and at the post-peak stage, where the dowels are more important. During a seismic event, an anchor may be subjected to a combination of cyclic tension and shear forces. Furthermore, the anchor may be located in a crack that forms during the earthquake. Specifically, the direction of application of the actions (axial, shear, combined), the state of the surrounding concrete, quantity, and orientation of reinforcement in the vicinity of the anchorage, and the characteristics of the anchor, including load transfer mechanism, material properties, diameter, and embedment (Eligehausen et al. 2006).

In order to study the contribution of dowels and to investigate further their design and placement, they were modelled in the FE model II and their modelling in DIANA FEA is presented in this section.

As discussed in Sect. 2.1.2.1, the frame was modelled with plane stress elements that do not have rotational degrees of freedom and the reinforcement elements that were used for the existing frame reinforcements and the web reinforcement of the infill wall can only take axial loads. As already stated, the local behaviour of dowels in the FE model is important in order to study their contribution. Therefore, the shear that the dowels carry in actual cases was important to be included in the FE model. In this way, for the FE model II, bond-slip beam-element reinforcements (BAR LINE, INTERF BEAM) that are available in the DIANA FEA element library as embedded lines in regular plane stress elements were used to capture the real behaviour of dowels in the FE model. The deformation of bond-slip reinforcements may not be the same as that of the elements in which they are located since relative slip is allowed. The reinforcement is connected with interface elements to the continuum elements in which it is located. Material and geometry properties are defined both for the reinforcement bar and for the bond-slip interface. Characteristics of the reinforcement are defined by the location, material, and dimensional properties. The type of the beam reinforcement element in plane-stress elements (mother element, CQ16M) that is internally used is automatically determined as CL9BE.

For the FE model II, three diameters (Y20, Y18, Y16) of circular beam elements with different lengths were used for the dowels, as shown in Table 3, and correspond to the ones

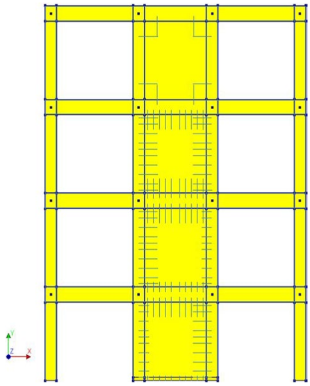

Fig. 2 Dowels geometry in the FE model

of the prototype model described in (Poljansek et al. 2014). The geometry of the dowels as added in the FE model II is shown in Fig. 2.

2.1.2.4 Interface mesh The interface area between the wall and the frame was modelled in the FE model II to capture the tension cut-off behaviour between the existing frame and the new infill wall. This allows for a more realistic contribution of the dowel's reinforcement bars to the resistance of the model. For the interface between the frame and the walls, the two-dimensional (2D) line interface (CL12I) from the DIANA element library was applied.

The structural interface elements describe the interface behaviour in terms of a relation between the normal and shear tractions and relative displacements across the interface (DIANA FEA BV 2019). The 2D line interface elements of the DIANA library that were applied were placed between the edges of the two-dimensional elements of concrete frame members and the concrete wall. For 2D line interface elements, the thickness (out-of-plane) is required to be specified by the user for plane stress. For the applied interface elements, the same thickness of plane stress elements of 250 mm was applied. For this type of 2D line interfaces elements, DIANA determines the direction in which the thickness is measured from the element shape.

2.1.2.5 Mass mesh As it is described in Poljansek et al., 2014, the SERFIN specimen was a full-scale prototype model and since the FE models of the south frame of the specimen that were generated are 2D models, the mass of half the weight (312 Tons) of the prototype building was added in the models by using the point mass elements (PT3T) on the 16 joints of the frame (see Fig. 1).

The point mass elements that were applied in the models, may be applied to add mass, or damping to the FE model without influencing the stiffness. The point elements do not have any post-analysis results like strains or stresses. As point mass, these elements are typically used to correct the deadweight or to affect the inertial mass in a dynamic analysis. For the generated FE models, the point mass elements were not applied to add damping to the FE model. They were applied to add mass without influencing the stiffness. Specifically, they were used to correct the deadweight of the simulated frame and to affect the inertial mass, since a dynamic analysis was then executed. In the specific case, the point mass was used in 2D elements, thus the direction without stiffness was supported.

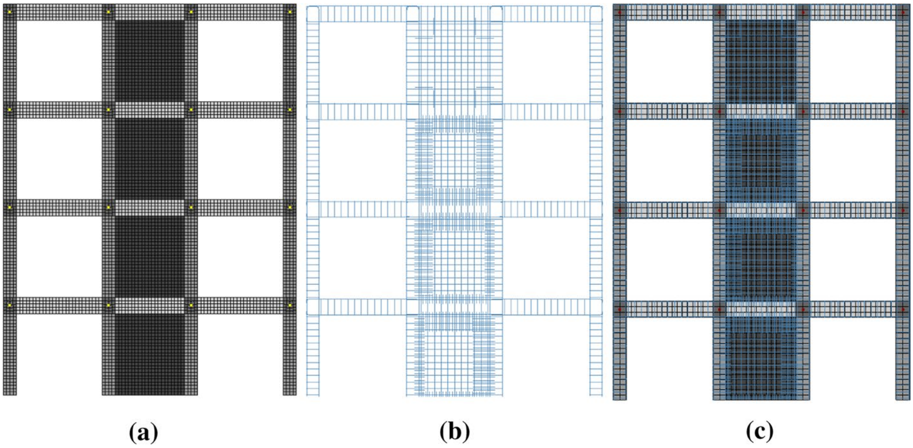

Fig. 3 **a** Monolithic RC frame with RC infills with plane stress elements, **b** Embedded reinforcement bars for the existing frame and web reinforcements and dowels, **c** Complete FE model I (DIANA FEA BV 2019)

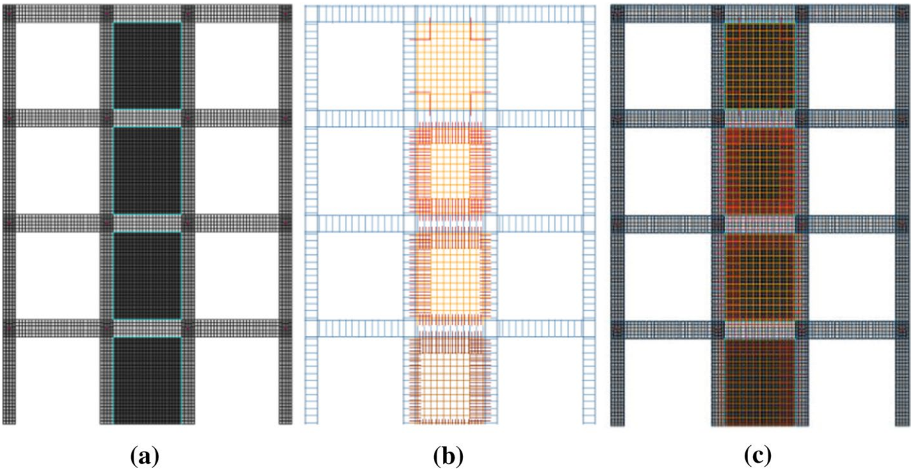

Fig. 4 **a** RC frame with 2D line interface elements at the interfaces and plane stress elements, **b** Embedded reinforcement bars for the existing frame and web reinforcements and dowel elements which can take shear forces, **c** Complete FE model II (DIANA FEA BV 2019)

2.1.2.6 Generated mesh The generated mesh of concrete members, reinforcement, interface areas, dowels, and mass points in the FE models that were developed in the environment of DIANA FEA are shown in Figs. 3 and 4 for the first and second models, respectively.

In Figure 3, the first 'monolithic' model that was generated is presented. As shown, all the concrete members were meshed with the plane stress elements, and the mass point elements are shown at the 16 joints of the frame. It is also shown that the frame, the web reinforcing bars, and the dowels were meshed as 1D embedded reinforcement in the plane stress elements.

In Figure 4, the second ‘non-monolithic’ FE model is presented. In Figure 4a, the plane stress elements that form the frame with the infill walls are illustrated along with the mass point elements at the joints of the frame. Added to that, in this model the 2D line interface elements between the new infill wall and the surrounding frame (blue lines) are shown. In Figure 4b, the frame reinforcing bars (in blue), the web reinforcement of the infill wall (in orange), and the dowels connecting the new infill wall to the surrounding frame (in red) are displayed. In Figure 4c, all the elements of the model that was developed are shown.

In Table 5, the elements that were selected from the DIANA FEA element library, and the parameters that were defined for the generation of their mesh are presented.

2.1.3 Material constitutive laws

The material models that were selected from the DIANA FEA material library for both concrete and reinforcement steel materials describe the hysteretic behaviour of materials under cyclic loading. More specifically, the constitutive laws of the materials model the stiffness and strength degradation and the material softening behaviour which causes localization and redistribution of strains in the structure (plasticity). The materials’ constitutive laws that were applied for all the materials of the developed FE models are described in this section.

2.1.3.1 Concrete constitutive law In this research, the behaviour of concrete was simulated through a material model which expresses the hysteretic behaviour of concrete under cyclic loading (stiffness and strength degradation), and it is described in this section. For the FE models that were developed, the ‘Total-strain based crack model’ with rotating crack orientation was used and the Maekawa cracked concrete model was applied for the compressive behaviour of concrete. For the behaviour of concrete in tension, the fib Model Code for Concrete Structures 2010 tensile curve was chosen. In the presented implementation, the behaviour in loading and unloading is modelled with a secant unloading in DIANA FEA (Fig. 5).

The Total-strain based crack model is founded on total strain and is formulated along the lines of the Modified Compression Field Theory, originally proposed by Vecchio and Collins (1986). For more information about the concept of smeared cracking see DIANA FEA BV (2019).

The rotating crack approach was selected for the developed FE model since it has been practiced in the constitutive modelling of reinforced concrete for a long time and appeared to be well suited for RC structures. A more detailed explanation of the Total Strain Crack model concept is given in DIANA FEA BV (2019).

For the Total Strain Crack model, several functions based on fracture energy are implemented, which are all related to a crack bandwidth as it is usually the case in smeared crack models (DIANA FEA BV 2019). For the developed FE model the nonlinear tension softening (Fig. 6) according to Paragraph 5.1.8.2 of the “fib Model Code for Concrete Structures 2010” (FIB 2013) was used to model the tensile behaviour of concrete, with the tensile strength (f_t) equal to 2.6 MPa.

For the compressive behaviour of concrete, the curve that was selected from the available hardening–softening curves in compression from the DIANA material library is the Maekawa Cracked Concrete curves (see Fig. 1). When the Maekawa Cracked Concrete curve is selected, automatically the unloading and reloading curves in both tension and compressive regime are applied in the Total Strain Crack model (DIANA FEA BV 2019). For this model, the compressive strength f_c under uniaxial stress situations is defined.

Table 5 Elements that were selected from the DIANA FEA element library and defined parameters

Members	Concrete	Reinforcement steel bars (frame and web reinforcement of infill walls)	Dowels	Interface	Mass
Applied elements	2D regular plane stress quadrilateral elements with 8 nodes '*CQ16M*'	Embedded bar reinforcement in plane stress elements	Bond-slip reinforcement with beam elements '*BAR LINE, INTERF BEAM*'	2D line interface elements '*CL12I*'	Point mass elements '*PT3T*' translation, point mass/damping, 1 node
Defined parameters	Thickness:*250 mm* Size:*100 × 100 mm*	Cross section-area of bars: *Y8, Y10, Y12, Y20*	Diameter of circle *Y16, Y18, Y20*	Thickness (width): *250 mm*	Half weight of the prototype building: *275,260 kg/16 points*

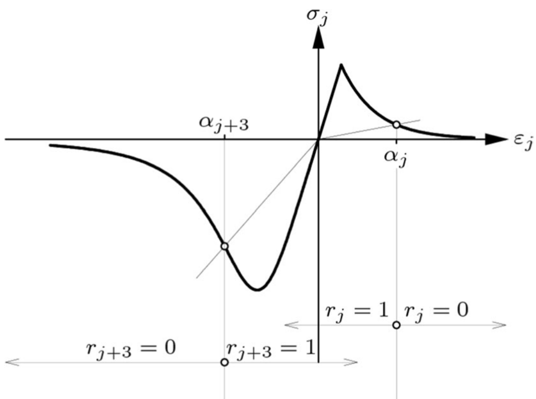

Fig. 5 Loading–unloading (DIANA FEA BV 2019)

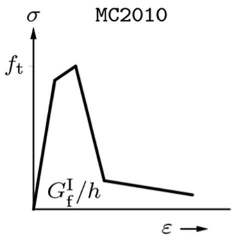

Fig. 6 Fib model code for concrete structures 2010 tensile behaviour of concrete (FIB 2013)

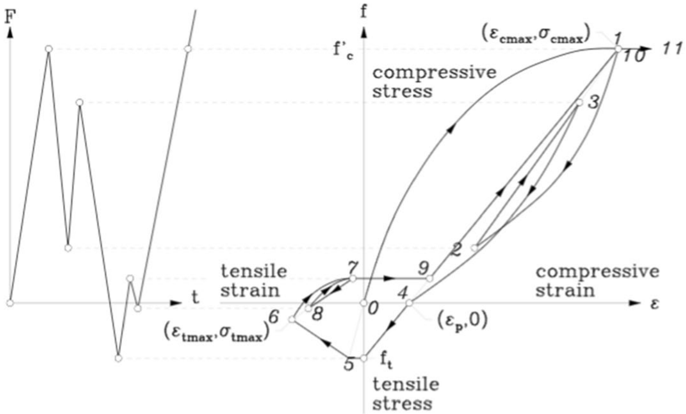

Fig. 7 Hysteresis for Maekawa model for compressive behaviour of concrete (Maekawa et al. 2003)

Young's modulus E is specified in the material properties and strain ε_c at the compressive strength in case of uniaxial loading conditions is calculated from Eq. 1 (DIANA FEA BV 2019). The reduction factor for the tensile strength Rf was set to linear, which specifies that the reduction factor of the tensile strength is equal to the damage factor K: $Rf = K$.

$$\varepsilon_c = 2.0\frac{f_c'}{E} \tag{1}$$

Figure 7 shows the typical uniaxial stress–strain development as defined by the Cracked Concrete curves. The equations that define the Maekawa Cracked Concrete curves can be found in Maekawa et al. (2003).

The direct input that is needed for the application of the Modified Maekawa model as implemented in the standard DIANA FEA code, is the Young's modulus, the Poisson's ratio, the selection of the total strain crack model (fixed, rotate, non-orthogonal), the compressive strength *fc* under uniaxial stress condition and the stress confinement function. In Table 6, the material mechanical properties of concrete that were defined in the model according to the SERFIN experimental concrete properties are shown. For the compressive behaviour of concrete, the Maekawa Cracked Concrete curve is used with a mean compressive strength of 33 MPa. It is important to mention that the Young's modulus of concrete was calibrated in the model to get the real behaviour of the building that was already cracked. Therefore, the Young's modulus was reduced from 30 to 15GPa. The validated parameters that were applied for the FE model are shown in Table 6. Moreover, a detailed description of the material constitutive model that was applied for concrete can be found in Maekawa et al. (2003).

The applied material model for concrete was assessed under cyclic loading to verify its hysteretic behaviour (by applying compressive and tensile force loads in one plane stress element) after the definition of the model parameters in the software. The stress–strain diagrams that were obtained from the DIANA FEA results and are illustrated in Fig. 8 reveal that the applied concrete model provides the hysteretic loops according to the defined tensile and compressive strengths in the FE model, while as shown, the model expresses the energy dissipation during cyclic loading paths according to the properties that were specified. As shown in Fig. 8 (on the right), in the tension region an initial short plateau and then a softening behaviour is shown when the strain reaches the value of $\varepsilon_{\mathrm{tu}} = 0.0002$ according to the model that was used to model the tensile behaviour of concrete (see Fig. 7).

2.1.3.2 Reinforcement constitutive law The classic explicit models for reinforcement steel modelling are Giuffre and Pinto (1970), Menegotto and Pinto (1973), Monti and Nuti (1991), and Monti and Nuti (1992). In the DIANA FEA material library, the Monti-Nuti, the Menegotto-Pinto, and the Dodd-Restrepo constitutive laws were available for cyclic loading. In this section, the applied constitutive law for reinforcement steel is presented and discussed.

The Menegotto-Pinto model (shown in Fig. 9) was employed to represent the hysteretic stress–strain behaviour of reinforcing steel elements of the existing frame and for the web reinforcements of the FE model II and the dowels of the FE model I. This model is based on isotropic plasticity, and it is a plasticity model for the cyclic behaviour of steel available for embedded reinforcements (DIANA FEA BV 2019). The parameters that are necessary to be specified are the yield stress, the elastic modulus, the hardening ratio, and the weighting coefficient in the case of buckling. The yield stress of the existing frame reinforcement was 400 MPa and the yield stress of the infill-wall web-reinforcement and dowels was 450 MPa same as in the specimen of the SERFIN experiment. The material properties that were defined for reinforcement bars in DIANA FEA are shown in Table 7.

The hysteretic behaviour of the steel model was examined in a 1D element (uniaxial) that was in a plane stress element by applying compressive and tensile loads. In this way, it

Table 6 Concrete material model parameters defined in DIANA FEA

Linear material properties		Total strain-based cracked model	Tensile behaviour “fib Model Code for Concrete Structures 2010”		Compressive behaviour “Maekawa cracked concrete curves”	
Young’s modulus (E)	15GPa (reduced)	Rotating crack orientation	Tensile strength	2.6 MPa	Compressive strength	33 MPa
Poisson’s ratio	0.2		Mode-I tensile fracture energy	136.98 N/m	Stress confinement	No increase
Mass density	2500 kg/m^3		Crack bandwidth specification	Rots		

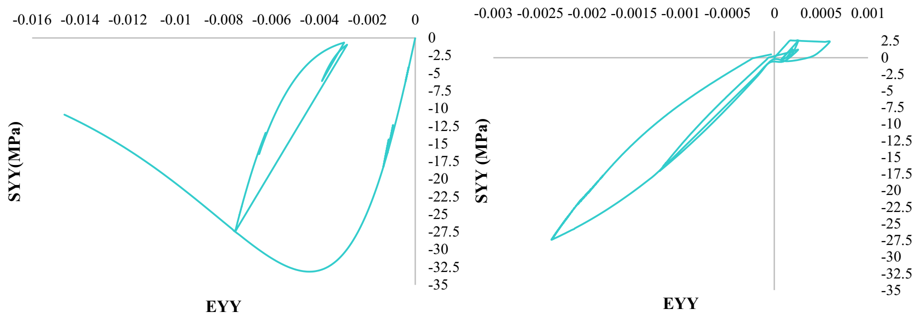

Fig. 8 Stress–strain diagrams derived from DIANA FEA for the applied concrete material

Fig. 9 Stress–strain relationship of the Menegotto-Pinto model (Faur and Mircea 2012)

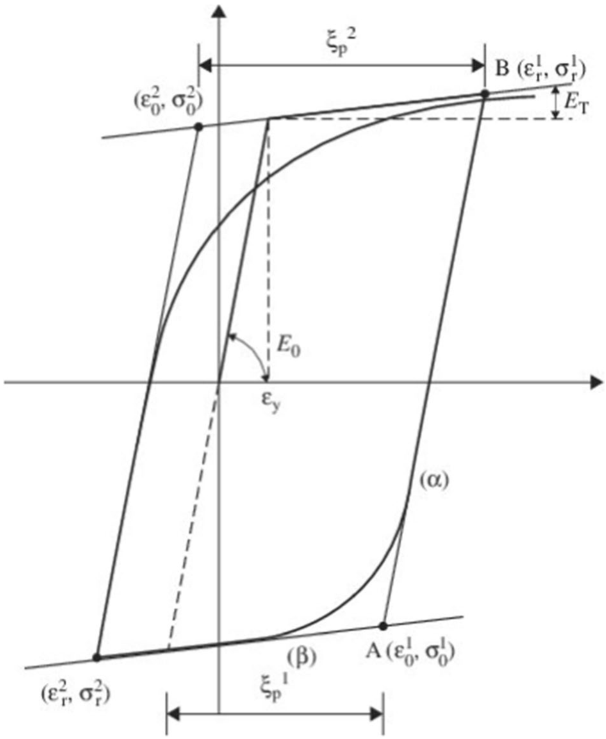

was ensured that the applied material model presents the actual behaviour of reinforcement steel under cyclic loading (see Fig. 10).

2.1.3.3 Dowels constitutive law A theoretical analysis of the resistance offered to a shearing force applied to the projecting end of a bar embedded in concrete was published by Timoshenko and Lessels in 1925. The bar was treated as a beam on an elastic foundation so that the support reaction on the embedded length was proportional to the transverse deflection. This approach was extended by others to the problem of dowel connections in

Table 7 Reinforcement steel material model parameters defined in DIANA FEA

Linear elasticity		Menegotto-Pinto	
Young's modulus (E)	*200GPa*	Yield stress	*400 MPa for frame members* *450 MPa for walls*
Mass density	*7800 kg/m³*	Initial tangent slope ratio	*0.05*
		Initial curvature parameter	*20*
		Constant a1	*20*
		Constant a2	*18.5*
		Constant a3	*0.02*
		Constant a4	*3*

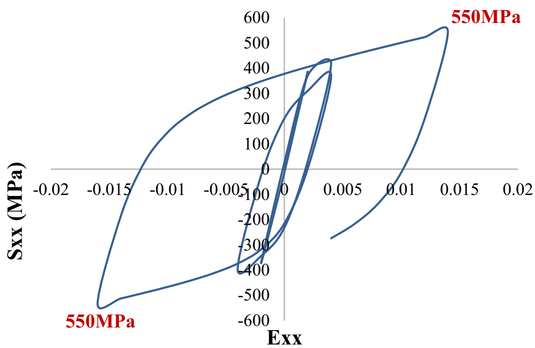

Fig. 10 Stress–strain diagram derived from DIANA FEA for Menegotto-Pinto model

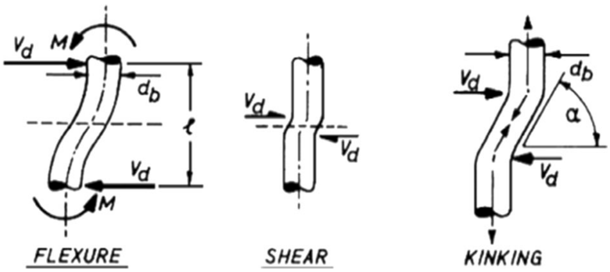

Fig. 11 Dowel action according to Paulay et al. (1974)

concrete road slabs and the criterion of failure was assumed to be the direct compressive stress beneath the dowel bar at the face of concrete, the limit of which was considered to the cylinder strength of concrete. Marcus (1951), however, found that in tests of dowel bars embedded in concrete the average bearing stress at failure was often more than twice the crushing strength, and suggested that the concrete criterion was the tensile strain causing splitting of the concrete below the dowel (Bennett and Banerjee 1976).

The actual behaviour of dowels under shear is shown in Figs. 11 and 12. according to (Paulay et al. 1974; Maitra et al. 2009). As explained earlier in this section, the

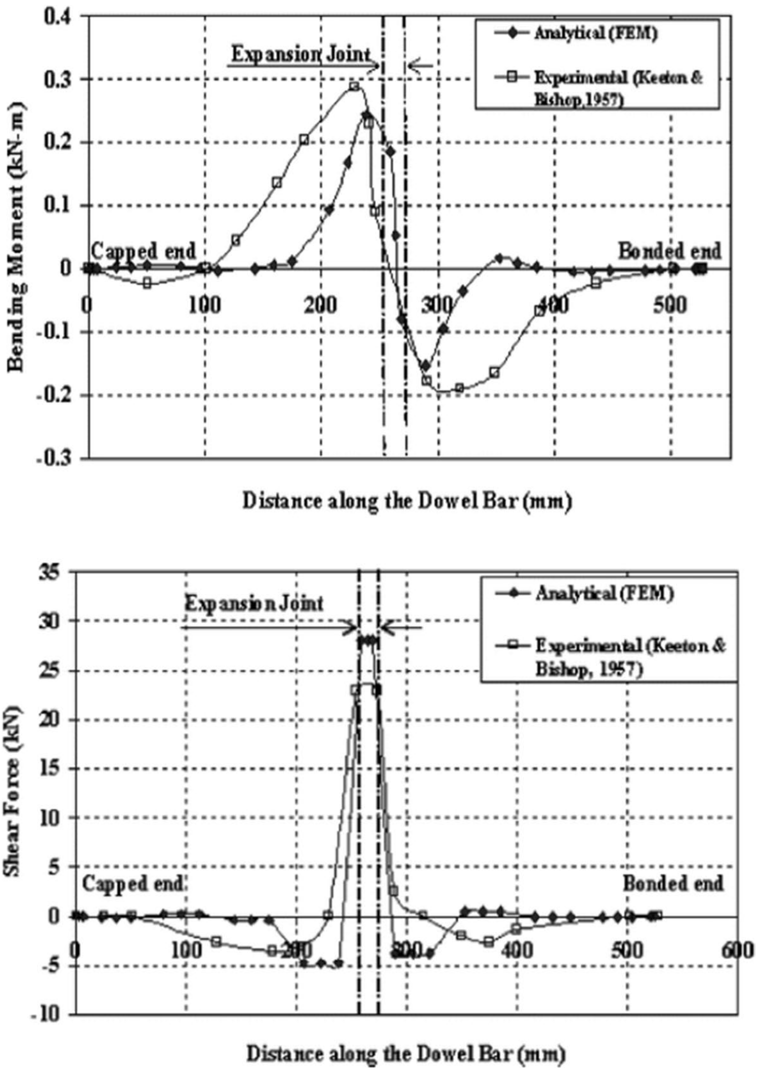

Fig. 12 Bending moment diagram for a dowel bar (up) and shear force diagram for a dowel (down) (Maitra et al. 2009)

application of dowels in DIANA was achieved through different modelling since the frame was modelled with plane stress elements that do not take shear forces or moments. So, for the dowels that were modelled to capture the shear stress in the FE model II, the Menegotto-Pinto model was replaced with the Von-Mises plasticity model since the latter can also be applied to control both axial and shear stresses for cyclic loading of the reinforcement, whereas the Menegotto-Pinto model is appropriate for the reinforcement elements that can solely take axial loads. As a result, it can only control the tensile and compressive stresses.

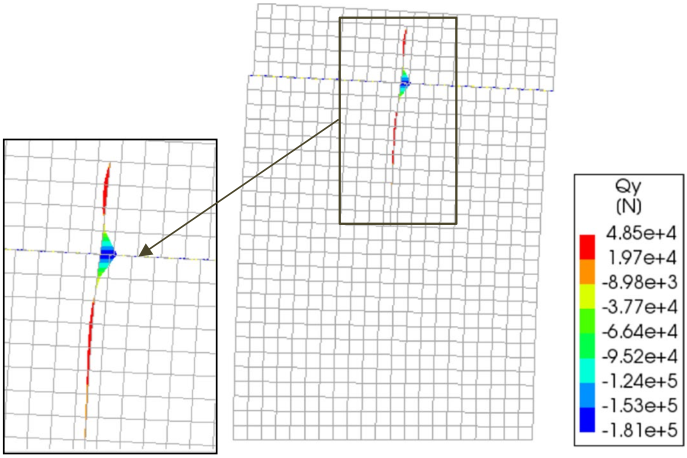

Fig. 13 Shear force diagram of dowel at the interface in DIANA FEA

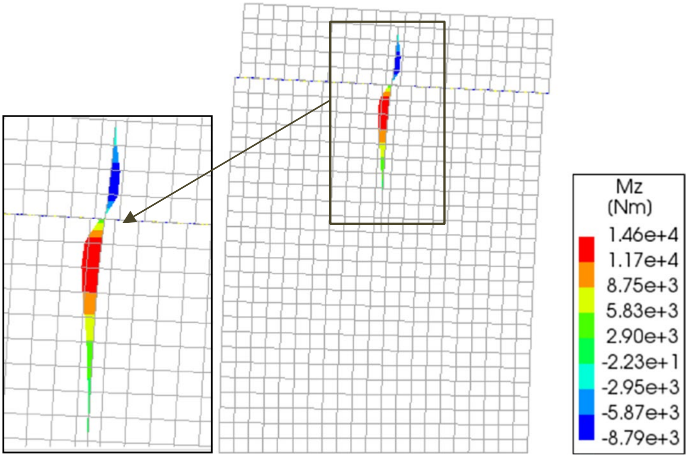

Fig. 14 Moment diagram of dowel at the interface in DIANA FEA

For the verification of the dowel's proper modelling in DIANA, a push-over test with a beam and a wall with an interface between them and a dowel was executed. In this test, the parameters of the Coulomb friction model that was applied at the interface (cohesion and friction) were set to zero, and only the gap criterion was applied. Therefore, the dowels would take all the shear force that was applied. As it is shown in Figs. 13 and 14, the expected moment and shear diagrams of dowels that were taken from the literature were obtained in the finite element model and the dowels took the shear force that was applied to the model. It is obvious that this model is close to reality and the expected moment and shear force diagrams of dowels according to the literature were captured. More specifically, in Figs. 13 and 14 it is shown that the maximum shear force and zero moments at the interface are like the diagrams that are given in the literature.

Table 8 Von-Mises plasticity model parameters defined in DIANA FEA

Linear elasticity	Von Mises plasticity nonlinear model	Bond-slip interface
Young's modulus (E)—200GPa	Yield stress—450 MPa	Normal stiffness modulus – 2e11N/m^3
Mass density—7800 kg/m^3	No hardening function	Shear stiffness modulus – 2e14N/m^3
		Bond-slip interface failure model – *Shima bond-slip function*
		Compression strength: 33 MPa
		Diameter per bar: 20, 18, 16
		Factor to shear-stress: 1

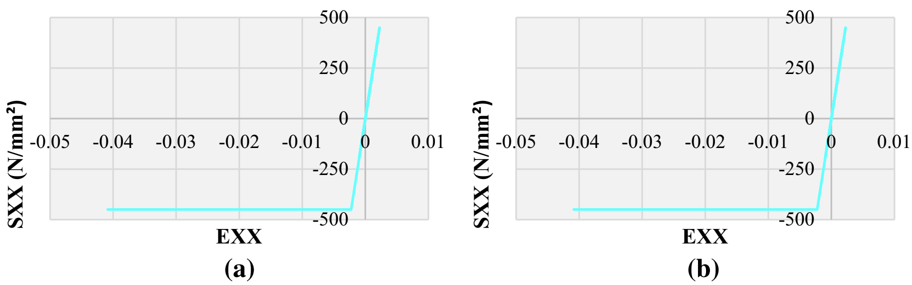

Fig. 15 Stress–strain diagram derived from DIANA FEA for Von-Mises plasticity model **a** reaching ultimate compressive stress **b** reaching ultimate tensile stress

The Von-Mises plasticity model parameters are presented in Table 8 as defined in the DIANA FE model. Also, the Von-Mises stress–strain diagram as specified in the DIANA FE model is shown in Fig. 15.

2.1.3.4 Interface constitutive law As mentioned before, the new infill wall and the bounding existing frame were constructed at different times and the actual actions of these areas should be properly modelled in the FE model. Specifically, the interface area between the new infill wall and the surrounding frame members should represent the cohesion and the friction between the interfaces. In addition, the dowel action should be active at the interface between the two members. The general concept of interface material modelling and the specific interface material model that was used from the DIANA FEA material library for the FE model II are presented and discussed in this section.

In general, the behaviour of an interface between two parts of a structure is governed by friction. This behaviour can be modelled with the Coulomb friction model. This model was used to represent the cohesion and the friction between the interfaces in FE model II, which at the same time provides the option of the gap criterion in the case of tensile stress between the two interfaces. To achieve this aim, the brittle gapping model was applied with very small tensile strength, in order to let the dowels carry the shear stresses at the interface. The linear material properties of the Coulomb friction model were set through trials to achieve the outcomes that were the closest to the results of the test specimen.

The Coulomb friction model is given by the yield surface and the plastic potential surface given in DIANA FEA BV (2019), where tan *(φ)* is the friction coefficient (also

Table 9 Coulomb friction model parameters defined in DIANA FEA

Linear material properties for "2D line interface"	Coulomb friction	Interface opening model "Gapping model"
Normal stiffness modulus-y *2000 N/m³*	Cohesion-*1e7Pa*	Tensile strength-*1e-6 Pa*
Shear stiffness modulus-x *2000 N/m³*	Friction angle-*0.5 rad*	Mode-II shear (model for gap appearance)—*Brittle*
	Dilatancy angle-*0 rad*	

commonly known by the symbol μ), and c the cohesion. It is important to mention that it is possible to extend the friction criterion with a gap criterion, where DIANA supposed that a gap arises if the tensile traction t_n normal to the interface exceeds a stated value. After a gap formation, t_n is immediately cut down to zero (brittle cracking). The full description and details of the Coulomb friction material model can be found in DIANA FEA BV (2019). The Coulomb friction criterion material properties that were defined for the FE model II are given in Table 9.

2.1.4 Loads

The loads that were applied in the FE model are presented in this section. The same values of dead and live loads with the SERFIN prototype model were applied on the beams as edge pressure load in the DIANA FEA model as is shown in Fig. 16. The earthquake signal Herzeg Novi accelerogram of the Montenegro earthquake in 1979 was scaled to 0.25 g acceleration and was applied as body force in the FE models for the base excitation with the earthquake time history function (shown in Fig. 17).

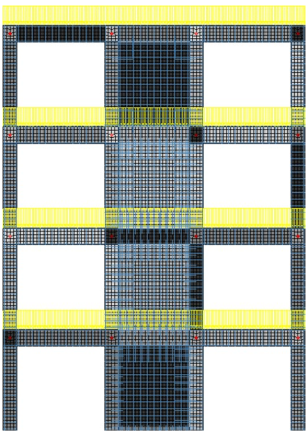

Fig. 16 Gravity vertical load applied in the FE model

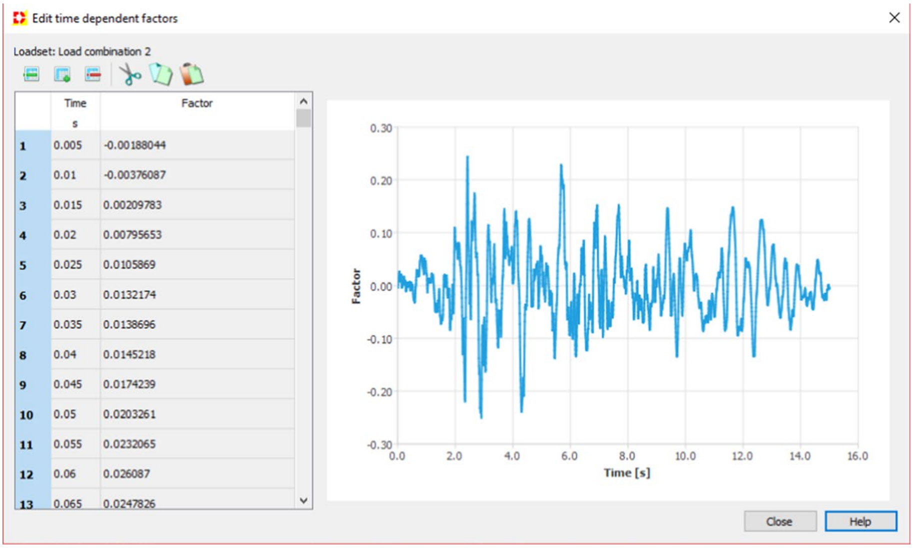

Fig. 17 Base excitation with time history function (0.25 g) applied in the FE model

2.1.5 Analysis

The analysis procedure that was executed in DIANA FEA, iterative methods and the convergence tolerance that were applied are discussed in this section. The analysis procedure that was executed in DIANA FEA was a structural physically nonlinear analysis with dynamic effects in order to execute the earthquake excitation load that was imposed.

The procedure of the completion of the nonlinear analysis was a time-consuming one, requiring a large number of trial-and-error attempts in order to complete an entire nonlinear transient analysis of the model. This was due to convergence issues that arose due to the highly nonlinear nature of the problem in hand that required updating and fine-tuning of the model parameters, and the tolerances of the convergence criteria.

Since the analysis that was executed in DIANA FEA was with transient effects, the consistent mass and damping matrix were calculated during the analysis with the Newmark time integration method (with Beta = 0.25 and Gamma = 0.5) in DIANA FEA. The Rayleigh damping *a* factor for the mass matrix and β factor for the stiffness matrix were calculated from the equations of the Rayleigh damping equation shown in Eq. 2. The Rayleigh factors were calculated for $\zeta = 0.25\%$, which is a small value, and this was chosen since the SERFIN experiment was a PsD and not a dynamic test, therefore there is no contribution of the velocity term of the dynamic equation during the test. To simulate this a small value of damping was chosen for the analysis of the frame in which the velocity term is present. The initial and the final frequencies of the SERFIN frame were used for the calculation of the factors as $F_i = 2.56$ Hz and $F_j = 99$ Hz.

$$C = \alpha M + \beta K \tag{2}$$

$$\alpha = \zeta * \left(2\omega_i\omega_j / \left(\omega_i + \omega_j\right)\right)$$

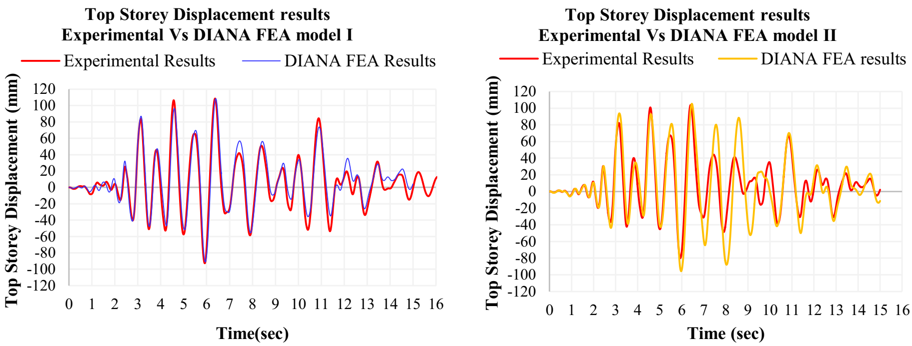

Fig. 18 Fourth storey displacements versus time (FE model I and II in left and right graphs, respectively)

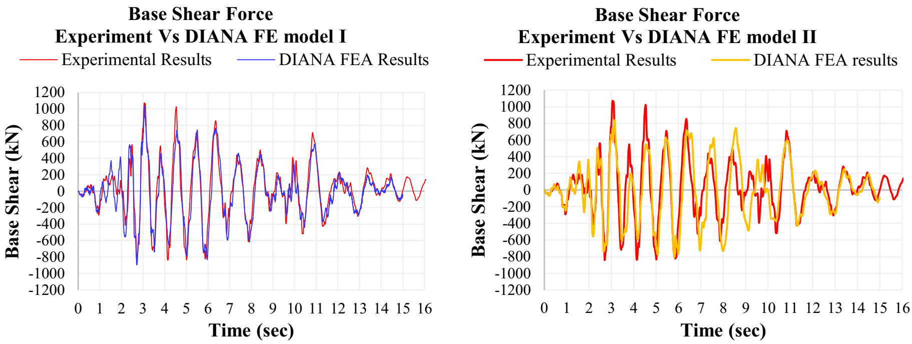

Fig. 19 Base shear force versus time (FE model I and II in left and right graphs, respectively)

$$\beta = \zeta * \left(2/\left(\omega_i + \omega_j\right)\right)$$

The iterative method that was applied for the equilibrium iteration for both FE models was the secant (quasi-newton), which is an implicit algorithm iterative method applied in addition to the line search method.

The convergence tolerance and time step that were applied for the two FE models were not the same. For the first FE model, the convergence tolerance that was applied was 1% for force and displacement. The time-step for the transient analysis was set to 0.005 s and in total there were 3000 steps executed since the imposed earthquake load had a duration of 15 s. For the second FE model, which was more demanding in analysis, the convergence tolerance was 0.2% for both forces and displacements. The time-step for the transient analysis was set to 0.002 s, so 7500 steps were executed for the completion of the analysis. A very demanding analysis was necessary especially for the second FE model because of the fine generated mesh, the nonlinear transient analysis procedures, the interfaces, and the modelling of the dowels.

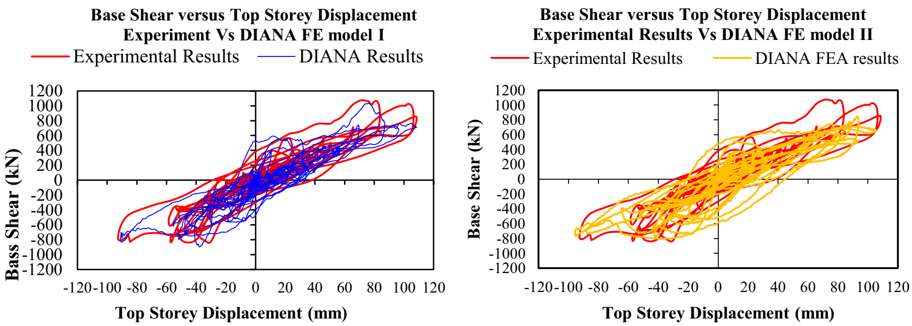

Fig. 20 Base shear force versus top-storey displacement (FE model I and II in left and right graphs, respectively)

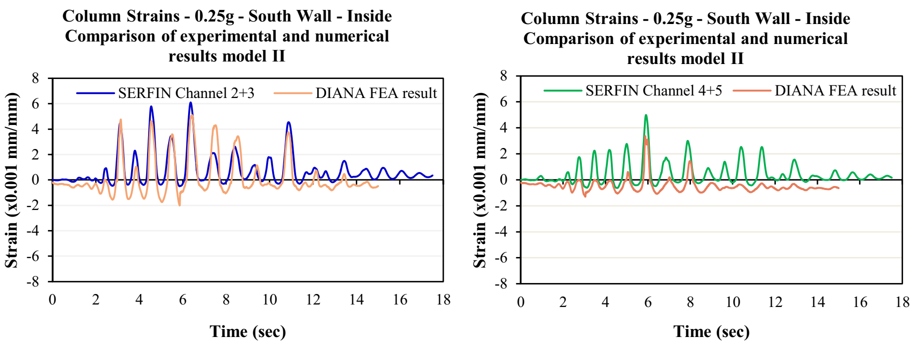

Fig. 21 Strain distribution on the ground floor bounding columns of the wall comparison between the experimental and numerical results using model II

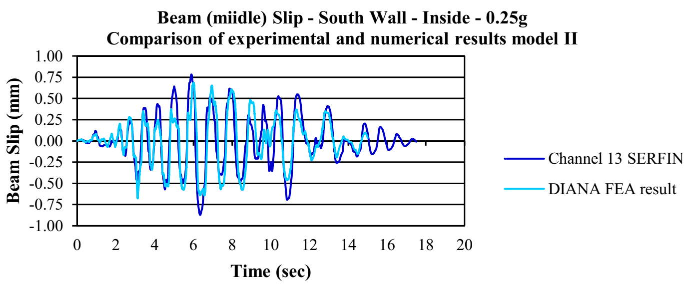

Fig. 22 Slip in the middle of the ground beam comparison between the experimental and numerical results using model II

3 Numerical calibration

In order to validate the FE model that was developed as explained in Sect. 2, the results of the south wall of the SERFIN experiment were compared with the DIANA FE model results. Initially, the first FE model (model I) was calibrated to capture the global

Fig. 23 The tensile stress of 2.6 MPa at 6.4 s (maximum displacement of the frame in the east direction) at the east column of the frame

experimental results, and then the second FE model (model II) was calibrated to capture both the global behaviour of the structures and the local behaviour of dowels. The comparison of the experimental results and the numerical results for the two FE models that are described in Sect. 2 is shown in Figs. 18, 19, 20, 21, 22 and 23.

3.1 Global results comparison

The response history of the top-storey displacements of the frame is compared in Fig. 18 and the response history of the base shear-force of the frame is compared in Fig. 19. Moreover, the top-storey displacement versus the base shear-force is compared in Fig. 20 in order to examine energy absorption and stiffness degradation of the model.

From the FE models' global results, it is apparent that both FE models are very close to the experimental results. As shown in Figs. 18 and 19 the peak values are captured for both the forces and the displacements, and it is clear that the FE models capture the frequency of the actual structure. In addition, the stiffness degradation is captured very well (Fig. 20). It is obvious that there is a good agreement between the real case study and numerical results for both models despite the number of influencing factors regarding the simulation and analysis, such as the type of elements, the mesh, the material models, the nonlinear time-history analysis, the iteration methods, and the convergence criteria. Even though model I captured the global monolithic behaviour of the real structure of the experiment very closely, it was not able to capture the interaction of RC infills with the surrounding frame, thus, the local results of the dowel action contribution at the interface could not be obtained from this model. So, in order to be able to complement the experimental results and to study the interaction between RC infills and bounding frame, both at the local and global level, by reducing the number of dowels used, the simulated model II proved to be suitable and reliable and was used to provide information for local results at any location on the RC infill wall or the interface between the wall and the bounding frame members. Model II simulated the RC infills and their interaction with the surrounding frame through the wall-frame interface, the dowel action and the starter bars contribution at the interface, while at the same time simulated well the global response of the full-scale SERFIN specimen.

3.2 Local results comparison

In this section, the local results that were taken from the SERFIN specimen are compared with the numerical results obtained from model II. The strain distribution on the ground floor columns of the wall (Fig. 21) and the slip displacement on the ground beam (Fig. 22) are compared with the numerical results. Moreover, from the experimental results, the main failures that occurred were the crack opening at the bottom of the column-wall on both sides of the wall and the failure of the east column at the bottom (Poljansek et al., 2014). These results are also compared with the DIANA FEA results in Fig. 23.

As shown in Figs. 21 and 22, the strain distribution on the bounding columns of the wall at the ground floor were captured in the FE model, as well as the slip in the middle of the ground beam of the wall. Also, the tensile forces in the outer column at the east side of the frame were captured in the FE model as shown in Fig. 23, where the tensile stress of concrete was reached on the east side of the column.

4 Conclusions

It is obvious that there is a good agreement between the real case study and the results of the 2D FE models, both model I and model II, despite the number of influencing factors regarding the simulation and analysis. It is important to mention that a very good calibration of the model was necessary regarding the nonlinear analysis parameters and methods and regarding the normal and shear stiffness modulus of the interface and bond-slip material models in order to get these results. This is because there are no clear values for these mechanisms since they are complicated, and their characteristics are difficult to measure in actual tests.

It can be concluded that the aim of developing a reliable model of RC infills and its interaction with the surrounding frame through the dowel action and starter bars contribution at the interface was achieved by the FE models presented in this paper, but in particular by model II, which was proved to be able to capture not only the global response as did model I, but also the local response of the infilled frame. Consequently, this sophisticated FE model, which fulfils the first action of this research, could be used to study the configurations with a reduced number of dowels to complement the experimental results and to study the interaction between RC infills and bounding frames both at the local and global levels, and hence fulfil the second action of this research. This calibrated model was used to perform a parametric study that covered a range between monolithic behaviour and infilled frame, by varying the number of dowels connecting the wall to the bounding frame. The results of this study, which will be presented in a subsequent publication, will contribute to the investigation of a general model for the application and the design of RC infills in existing RC frames.

References

Agarwal P, Shrikhande M (2006) Earthquake resistant design of structures, 2nd edn. Prentice-Hall of India Private Limited, Eastern Economy Edition, New Delhi

Almusallam TH, Al-Salloum YA (2007) Behavior of FRP strengthened infill walls under in-plane seismic loading. J Compos Const 11:308–318

Altin S, Ersoy U, Tankut T (1992) Hysteretic response of reinforced concrete infilled frames. J Struct Div 118(8):2133–2150

American Society of Civil Engineers (ASCE) (2007) Seismic rehabilitation of existing buildings, ASCE/SEI 41-06. https://doi.org/10.1061/9780784408841

Aoyama H, Kato D, Katsumata H, Hosokawa Y (1984) Strength and behavior of postcast shear walls for strengthening of existing R/C buildings. In: Proceeding Of the Eighth World conference on Earthquake Engineering (8WCEE), San Francisco, Calif., 1, pp 485–492

Baran M, Tankut T (2011) Experimental study on seismic strengthening of reinforced concrete frames by precast concrete panels. ACI Struct J 108:227–237

Bennett EW, Banerjee S (1976) Strength of beam-column connections with dowel reinforcement. Struct Eng 54(4):133–139

CEN (2010) Assessment and retrofitting of buildings : Eurocode 8 : design of structures for earthquake reistance : Part 3 : Assessment and retrofitting of buildings / European Committee for Standardization ; editor Cyprus Organisation of Standardisation. Brussels : European Committee for Standardization, c2010. https://vpn.cut.ac.cy/

Choi SH, Hwang JH, Han SJ, Joo HE, Yun H. Do, Kim KS (2020) Seismic performance assessments of RC frame structures strengthened by external precast wall panel. Appl Sci. https://doi.org/10.3390/app10051749

Chrysostomou CZ, Poljansek M, Kyriakides N, Taucer F, Molina FJ (2013a) Pseudo-dynamic tests on a full-scale four-storey reinforced concrete frame seismically retrofitted with reinforced concrete infilling. Struct Eng Int 23(2):159–166. https://doi.org/10.2749/101686613X13439149156831

Chrysostomou CZ, Kyriakides N, Poljansek M, Taucer F, Molina FJ (2013b) RC infilling of existing RC structures for seismic retrofitting. In: Ilki A, Fardis M (eds) Seismic evaluation and rehabilitation of structures. Geotechnical, geological and earthquake engineering, vol 26, pp 303–328. https://doi.org/10.1007/978-3-319-00458-7_17

Chrysostomou CZ, Kyriakides N, Kotronis P, Georgiou E (2014) RC infilling of existing RC structures for seismic retrofitting. In: Proceedings: Second European Conference on Earthquake Engineering and Seismology, Istanbul, Turkey

Chrysostomou CZ, Kyriakides N, Kotronis P, Georgiou E (2016) Derivation of fragility curves for RC frames retrofitted with RC infill walls based on full-scale pseudodynamic testing results. ECCOMAS Congress 2016, Paper 16727

DIANA FEA BV (2019) DIANA - finite element analysis. DIANA FEA BV

El-Ariss B (2007) Behavior of beams with dowel action. Eng Struct 29(6):899–903. https://doi.org/10.1016/j.engstruct.2006.07.008

Eligehausen R, Mallée R, Silva J (2006) Anchorage in Concrete Construction, First edition. In: Ernst & Sohn Verlag für Architektur und technische Wissenschaften GmbH & Co. KG, Berlin. ISBN:9783433011430. https://doi.org/10.1002/9783433601358

Fardis MN, Schetakis A, Strepelias E (2013) RC buildings retrofitted by converting frame bays into RC walls. Bull Earthq Eng. https://doi.org/10.1007/s10518-013-9435-6

Fardis MN (2009) Seismic design, assessment and retrofitting of concrete buildings. Based on EN-Eurocode 8. In: Geotechnical, geological, and earthquake engineering, Vol 8. Springer. ISBN 978-1-4020-9841-3. https://doi.org/10.1007/978-1-4020-9842-0

Faur A, Mircea C (2012) Numerical investigation of the nonlinear cyclic behavior of special reinforcing bars for precast concrete frames with hybrid connections. Acta Technica Napocensis: Civil Eng Architect 55(3):213–223

Fédération internationale du béton/International Federation for Structural Concrete (FIB) (2013) *fib* model code for concrete structures 2010, 1st edn. Wiley Library. ISBN: 978-3-433-03061-5. https://doi.org/10.1002/9783433604090

Frosch RJ (1996) Seismic rehabilitation using precast infill walls. University of Texas, Austin

Frosch RJ (1999) Panel connections for precast concrete infill walls. ACI Struct J 96:467–472

Frosch RJ, Li W, Jirsa JO, Kreger ME (1996) Retrofit of non-ductile moment-resisting frames using precast infill wall panels. Earthq Spectra 12(4):741–760

Giuffre A, Pinto P (1970) Reinforced concrete behavior under strong repeated loadings. Giornale Del Genio Civile 5:391–408

Jirsa JO (1988) Behavior of epoxy-grouted dowels and bolts used for repair or strengthening of RC structures. VII pp. 371–376.

KANEPE (2017) Code for intervention in reinforced concrete buildings, earthquake plannig and protection organization. Greek Retrofitting Code. Edited by Greek Organization for Seismic Planning and Protection (OASP). Greek Ministry for Envir. Plan. & Public Works, Athens, Greece

Kaplan H, Yilmaz S, Cetinkaya N, Atimtay E (2011) Seismic strengthening of RC structures with exterior shear walls. Sadhana 36(1):17–34

Koutas L, Bousias SN, Triantafillou TC (2015) Seismic strengthening of masonry-infilled RC frames with TRM: experimental study. Compos Const 19(2). https://doi.org/10.1061/(ASCE)CC.1943-5614.0000507

Kyriakides N, Chrysostomou CZ, Kotronis P, Georgiou E, Roussis P (2015) Numerical simulation of the experimental results of a RC frame retrofitted with RC Infill walls. Earthq Struct 9(4):735–752. https://doi.org/10.12989/eas.2015.9.4.735

Maekawa K, Okamura H, Pinanmas A (2003) Nonlinear mechanics of reinforced concrete, 1st edn. CRC Press London

Maitra SR, Reddy KS, Ramachandra LS (2009) Load transfer charactesistics of dowel bar system in jointed concrete pavement. Transp Eng. https://doi.org/10.1061/(ASCE)TE.1943-5436.0000065

Marcus H (1951) Load carrying capacity of dowels at transverse pavement joints. J Am Concr Inst 48(2):169–184

Menegotto M, Pinto PE (1973) Method of analysis for cyclically loaded RC frames including changes in geometry and nonelastic behaviour of elements under combined normal force and bending. In: IABSE Congress Reports of the Working Commission Band13

Moehle JP (2000) State of research on seismic retrofit of concrete building structures in the US. In: US-Japan Symposium and Workshop on Seismic Retrofit of Concrete Structures

Monti G, Nuti C (1991) Analytical model of cyclic behavior of reinforcing bars with inelastic buckling. Report No. 6/91 Dept. of Struct. Engrg. Rome, Italy

Monti G, Nuti C (1992) Nonlinear cyclic behavior of reinforcing bars including buckling. J Struct Eng 118(12):3268–3284

Ozden S, Akguzel U, Ozturan T (2011) Seismic strengthening of infilled reinforced concrete frames with composite materials. ACI Struct J 108:414–422

Paulay T, Park R, Phillips MH (1974) Horizontal construction joints in cast-in place reinforced concrete. American Concrete Institute (ACI) Special Publication Issue: 42-2 Shear in Reinforced Concrete, II(S.), vol 1. Farmington Hills, pp 599–616

Poljansek M, Taucer F, Molina J, Chrysostomou CZ, Kyriakides N, Onoufriou T, Roussis P, Kotronis P, Kosmopoulos A (2014) Seismic retrofitting of RC frames with RC infilling (SERFIN Project). Doi: https://doi.org/10.2788/630

Radomir Folici PP (2015) Seismic strengthening of buildings with RC walls. In: First Scientific-Applied Conference with International Participation Reinforced Concrete and Masonry Structures

Sonuvar MO, Ozcebe G, Ersoy U (2004) Rehabilitation of reinforced concrete frames with reinforced concrete infills. ACI Struct J 101(4):494–500

Strepelias I, Fardis M, Bousias S, Palios X, Biskinis D (2012) RC frames infilled ino RC walls for seismic retrofitting: design, experimental behaviour and modelling (Issue SEE 2012-02)

Sugano S (1980) A seismic strengthening of existing reinforced concrete buildings. In: Proceeding of the First Seminar on Repair and Retrofit of Structures

Turk AM, Ugur E, Ozcebe G (2006) Effect of introducing RC infill on seismic performance of damaged RC frames. Struct Eng Mech 23(5):469–486

Vecchio FJ, Collins MP (1986) The modified compression field theory for reinforced concrete elements subjected to shear. ACI J Proc 83(22):219–231

Wyllie LAJ (1988) Guidelines for epoxy grouted dowels in seismic strengthening projects. In: Proceeding of Ninth World Conference on Earthquake Engineering, Tokyo-Kyoto, Japan, vol VII, pp 499–504